Age of Correct Sensing in Sensing-and-then-transmit ISAC Networks

Yiyang Ge, Ke Xiong, *Member, IEEE*, Wenjuan Yu, *Senior Member, IEEE* Qiang Ni, *Senior Member, IEEE*, Wei Chen, *Senior Member, IEEE*, Pingyi Fan, *Senior Member, IEEE*, and Khaled Ben Letaief, *Fellow, IEEE*

***Abstract*—This paper investigates the sensing-and-then-transmit (SAT) integrated sensing and communication (ISAC) network, where a multi-functional base station (MBS) senses the target's state and then transmits the sensed results to the receiving node (RN). To measure the timeliness of the SAT process, we define a novel metric called Age of Correct Sensing (AoCS). To enhance the system's AoCS, we propose a pipelined SAT ISAC (P-SAT ISAC) paradigm, where the MBS simultaneously transmits individual beams to perform sensing and communication. We derive the mathematical expression of the probability of detection (PD), the probability of false alarm (PFA), and the probability of communication outage (PCO), based on which, the AoCS of the P-SAT ISAC is quantified. Furthermore, we formulate an expected AoCS minimization problem by optimizing the power splitting factor for sensing and communication to explore the achievable lower bound of AoCS. Then, the minimum expected AoCS is found by developing a linear search based algorithm. Simulation results validate the theoretical analysis on PD, PFA, and PCO, and also show the impact of system parameters on them, as well as the minimum achievable expected AoCS. Compared with the existing alternating SAT ISAC (A-SAT ISAC), our proposed P-SAT ISAC achieves an average reduction in expected AoCS of 38.97%, demonstrating the efficiency of the proposed pipelined sensing and communication paradigm in improving system timeliness.**

***Index Terms*—6G, integrated sensing and communications, age of information (AoI), resource allocation.**

This work was supported in part by the National Natural Science Foundation of China (NSFC) under Grant 62571028 and 62261160390, in part by the Changping Innovation Joint Fund of Beijing Natural Science Foundation under Grant L234084, and also in part by the Hong Kong Research Grant Council under the Area of Excellence (AoE) Scheme Grant No. AoE/E-601/22-R. *(Corresponding author: Ke Xiong.)*

Yiyang Ge and Ke Xiong are with the Engineering Research Center of Network Management Technology for High Speed Railway of the Ministry of Education, School of Computer and Information Technology, Beijing Jiaotong University, Beijing 100044, China, with the Collaborative Innovation Center of Railway Traffic Safety, Beijing Jiaotong University, Beijing 100044, China and also with the National Engineering Research Center of Advanced Network Technologies, Beijing Jiaotong University, Beijing 100044, China. (e-mail: yiyangge{kxiong}@bjtu.edu.cn).

Wenjuan Yu and Qiang Ni are with the School of Computing and Communications and Data Science Institute, Lancaster University, Lancaster LA1 4WA, U.K. (e-mail: w.yu8{q.ni}@lancaster.ac.uk).

Wei Chen and Pingyi Fan are with the Department of Electronic Engineering, State Keylab-oratory of Space Network and Communications, Beijing National ResearchCenter for Information Science and Technology, Tsinghua University, Beijing100084, China (email: wchen{fpy} @tsinghua.edu.cn).

Khaled Ben Letaief is with the Department of Electrical and Computer Engineering, Hong Kong University of Science and Technology (HKUST), Hong Kong, China (e-mail: eekhaled@ust.hk).

I. Introduction

THE emerging paradigm of Integrated Sensing and Communication (ISAC) has been recognized as a promising technology for 6G, aiming to provide ubiquitous, intelligent, and diverse services [1]. ISAC allows wireless systems to sense the surrounding environment and transmit data by sharing the same network resources [2].

Among various ISAC networks, the sense-and-then-transmit (SAT) ISAC network is emerging as a new typical paradigm and attracts increasing attention [3]. In SAT ISAC, a multi-functional base station (MBS) senses the target's state and then transmits the sensed results to the receiving node (RN) via beams. So far, two types of SAT paradigms, i.e., alternating SAT ISAC (A-SAT ISAC) and monobeam SAT ISAC (MB-SAT ISAC), have been presented in [4]. In A-SAT ISAC, the MBS transmits either a communication or a sensing beam in each time slot, where sensing and communication are performed sequentially. In MB-SAT ISAC, the MBS transmits one multi-functional beam in each slot to simultaneously perform sensing and communication, where the transmitted signal in the current slot carries the sensed result collected in the previous slot.

To date, ISAC has been designed for various scenarios, including autonomous driving and industrial automation, in which timeliness plays a critical role [5]–[7]. If the information is received after it becomes outdated, the actual state may have already changed, potentially leading to errors or even critical failures in time-sensitive applications. Recently, the age of information (AoI) has been proposed as a metric to quantify timeliness, and some works have been devoted to enhancing AoI performance in A-SAT ISAC networks, see e.g. [8]–[10]. In [8], AoI was used to quantify the timeliness of sensing and communication, and the average AoI of the sensing task was minimized in an A-SAT ISAC system. In [9], AoI was used to characterize the timeliness of sensing, communication, and computation, and the amount of sensing data was maximized with a maximum AoI constraint in an A-SAT ISAC system. In [10], AoI was used to jointly capture sensing accuracy and transmission timeliness, and the AoI of sensing updates was minimized in an A-SAT ISAC system.

It is worth noting that, to enhance the timeliness of SAT ISAC systems, correct sensed data should be transmitted as soon as possible. Nevertheless, in [8]–[10], sensing and communication were performed sequentially, so that the RN could only receive updated information once every two slots, leading to limitations in enhancing timeliness. Although, MB-SAT

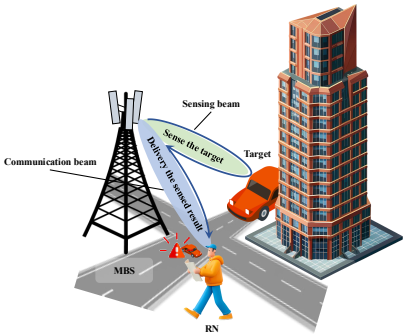

Fig. 1: An SAT ISAC-assisted intersection safety warning system.

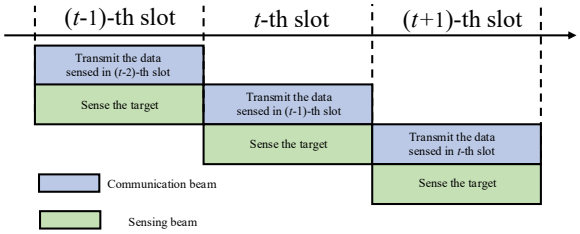

Fig. 2: Per-slot operation of the MBS.

ISAC allows the MBS to perform sensing and communication simultaneously within the same slot, employing mono beam to serve both sensing and communication may not be efficient, because sensing and communication have different objectives, making it challenging to simultaneously achieve high sensing and communication performance with mono beam design.

To fill this gap, this paper also investigates the SAT ISAC. To efficiently measure the timeliness of the SAT process, we define a novel metric, i.e., Age of Correct Sensing (AoCS). To promote the system's AoCS, we propose a pipelined SAT ISAC (P-SAT ISAC) paradigm. Closed-form expressions for the probability of detection (PD), probability of false alarm (PFA), and probability of communication outage (PCO) are derived, based on which, the long-term expected AoCS is quantified. To minimize the AoCS, we formulate an optimization problem by optimizing the power splitting factor and then the minimal AoCS is achieved by a linear-search algorithm. Simulation results validate the theoretical analysis on PD, PFA, and PCO, and further show the impact of system parameters on these metrics and on the minimum achievable AoCS. Moreover, compared with the existing A-SAT ISAC, our proposed P-SAT ISAC achieves an average 38.97% reduction in expected AoCS, demonstrating its effectiveness in enhancing information timeliness.

II. System Model

As illustrated in Fig. 1, we consider an SAT ISAC-assisted intersection safety warning system[1] configured as a downlink multiple-input single-output (MISO) network. The system comprises an MBS equipped with N_t transmitting and N_r receiving antennas, both configured as horizontal uniform linear arrays (ULAs), a single-antenna RN, and a target to be detected. The system operates in a time-slotted manner to enable synchronized detection and reporting. To enhance the system timeliness, we present a P-SAT ISAC paradigm illustrated in Fig. 2, where the MBS transmits two individual beams to perform sensing and communication in parallel within each time slot, where the sensing beam detects the target's state in the current slot while the communication beam transmits the sensed result obtained in the previous slot to the RN.

To perform sensing and communication simultaneously, the MBS employs a joint precoding vector denoted as a communication beamformer $\mathbf{w}_{\mathrm{c}} \in \mathbb{C}^{N_t \times 1}$ and a sensing beamformer $\mathbf{w}_{\mathrm{s}} \in \mathbb{C}^{N_t \times 1}$. Let P denote the total transmit power of MBS and $\rho_S \in [0,1]$ denote the power splitting factor. $\rho_S P$ is assigned for sensing and $(1-\rho_S)P$ for communication. Moreover, to enable correct sensing, the MBS collects L signal sequence [11] and [12]. Denote the sensing sequence as $\mathbf{s}_{\mathrm{s}} \in \mathbb{C}^{L\times 1}$ and the communication sequence as $\mathbf{s}_{\mathrm{c}} \in \mathbb{C}^{L\times 1}$, both of which are independent and identically distributed (i.i.d.) complex Gaussian random variables with zero mean and unit variance. Thus, the transmitted signal $\mathbf{X}$ is given by $\mathbf{X} = \sqrt{\rho_{\mathrm{s}} P}\,\mathbf{w}_{\mathrm{s}}\mathbf{s}_{\mathrm{s}}^H + \sqrt{(1-\rho_{\mathrm{s}})P}\,\mathbf{w}_{\mathrm{c}}\mathbf{s}_{\mathrm{c}}^H$.

A. Target Detection

To characterize the dynamic evolution of the target, we model the sensing environment as a discrete-time two-state Markov process [13]. Let $X(t) \in \{\mathcal{H}_0, \mathcal{H}_1\}$ denote the states of the target at time slot t, where $\mathcal{H}_0$ represents that the target is absent and $\mathcal{H}_1$ indicates that it is present. The target stays in $\mathcal{H}_0$ with probability p and in $\mathcal{H}_1$ with probability q. The target transitions from $\mathcal{H}_0$ to $\mathcal{H}_1$ with probability $(1-p)$, and from $\mathcal{H}_1$ to $\mathcal{H}_0$ with probability $(1-q)$, respectively. When the target is present, it reflects the sensing signal back to the MBS; otherwise, the MBS receives only noise. Thus, in the case of the target being present, the received signal is $\mathbf{Y} = \mathbf{G}\mathbf{X} + \mathbf{N} \in \mathbb{C}^{N_r \times L}$, where $\mathbf{G} \in \mathbb{C}^{N_r \times N_t}$ is the target reflection matrix, $\mathbf{X}$ is the transmit signal, and $\mathbf{n} = [\mathbf{n}(1), \cdots, \mathbf{n}(L)]$ denotes the noise (AWGN), where $\mathbf{n}(i) \sim \mathcal{CN}(\mathbf{0}, \sigma^2\mathbf{I})$ is a N_r dimensional i.i.d. complex Gaussian noise vector. The target reflection matrix is modeled as $\mathbf{G} = G_{\mathrm{s}}\alpha\beta_{\mathrm{s}}\mathbf{a}_{\mathrm{r}}(\theta_{\mathrm{tar}})\mathbf{a}_{\mathrm{t}}^T(\theta_{\mathrm{tar}})$, where $G_{\mathrm{s}} = \sqrt{N_r N_t}$ represents the sensing antenna gain, α is the radar cross section (RCS) coefficient, β_{s} is the path loss coefficient, and θ_{tar} is the angle of the target with respect to the MBS. The transmit and receive steering vectors of the target are defined as $\mathbf{a}_t(\theta_{\mathrm{tar}}) = \frac{1}{\sqrt{N_t}}\left[e^{-j\frac{N_t-1}{2}\pi\sin(\theta_{\mathrm{tar}})}, \ldots, e^{j\frac{N_t-1}{2}\pi\sin(\theta_{\mathrm{tar}})}\right]^T$ and $\mathbf{a}_r(\theta_{\mathrm{tar}}) = \frac{1}{\sqrt{N_r}}\left[e^{-j\frac{N_r-1}{2}\pi\sin(\theta_{\mathrm{tar}})}, \ldots, e^{j\frac{N_r-1}{2}\pi\sin(\theta_{\mathrm{tar}})}\right]^T$, respectively. When the target is absent, the received signal consists

[1]The proposed network model has many practical applications. For example, in intelligent transportation systems, a typical application is the SAT ISAC-assisted intersection safety warning. Specifically, in each slot, the MBS transmits a sensing beam and a communication beam, both sensing and communication beams jointly enable target detection, and the communication beam conveys the most recent sensing result to the RN. When a vehicle suddenly approaches, the system delivers an emergency notification to users' terminal devices; when no vehicles are detected, the system informs users that it is safe to cross.

of noise only, i.e., $\mathbf{Y} = \mathbf{N}$. With receiving beamforming $\mathbf{v} \in \mathbb{C}^{N_r \times 1}$, the processed signal is expressed by

$$\mathbf{r} = \begin{cases} \mathbf{v}^H \mathbf{N}, & \mathcal{H}_0, \\ \mathbf{v}^H \mathbf{G}\mathbf{X} + \mathbf{v}^H \mathbf{N}, & \mathcal{H}_1. \end{cases} \tag{1}$$

To achieve a simple system design close to practical deployment, similar to [10], the maximum ratio transmission (MRT)-based transmit beamforming and maximum ratio combining (MRC)-based receive beamforming are adopted for target sensing and communication. To detect the target, the sensed result is evaluated based on the likelihood ratio test (LRT) function, $\Lambda(\mathbf{r}) = \frac{p(\mathbf{r}|\mathcal{H}_1)}{p(\mathbf{r}|\mathcal{H}_0)}$. With Gaussian noise, the conditional probability density functions (PDF) of $\mathbf{r}$ are given by $p(\mathbf{r} \mid \mathcal{H}_0) = \frac{1}{(\pi\sigma^2)^L} \exp\left(-\frac{\|\mathbf{r}\|^2}{\sigma^2}\right)$ and $p(\mathbf{r} \mid \mathcal{H}_1) = \frac{1}{(\pi\sigma^2)^L} \exp\left(-\frac{\|\mathbf{r}-\mathbf{v}^H\mathbf{G}\mathbf{X}\|^2}{\sigma^2}\right)$. To be efficient, we use the logarithm form of $\Lambda(\mathbf{r})$ for target detection, which is

$$\begin{aligned} \ln \Lambda(\mathbf{r}) &= \tfrac{1}{\sigma^2}\left(\|\mathbf{r}\|^2 - \|\mathbf{r} - \mathbf{v}^H\mathbf{G}\mathbf{X}\|^2\right) \\ &= \tfrac{1}{\sigma^2}\left(2\Re(\mathbf{v}^H\mathbf{G}\mathbf{X}\mathbf{r}^H) - \|\mathbf{v}^H\mathbf{G}\mathbf{X}\|^2\right). \end{aligned} \tag{2}$$

Based on LRT, PD and PFA are defined as

$$\begin{cases} P_{\mathrm{D}} = \Pr\left\{\ln \Lambda(\mathbf{r}) \geq \gamma_{\mathrm{th}}^{\mathrm{sen}} \mid \mathcal{H}_1\right\}, \\ P_{\mathrm{FA}} = \Pr\left\{\ln \Lambda(\mathbf{r}) \geq \gamma_{\mathrm{th}}^{\mathrm{sen}} \mid \mathcal{H}_0\right\}, \end{cases} \tag{3}$$

where $\gamma_{\mathrm{th}}^{\mathrm{sen}}$ is the detection threshold.

B. The Probability of Communication Outage

Denote the channel between the MBS and the RN be $\mathbf{h} = G_{\mathrm{c}}\sqrt{\beta_{\mathrm{c}}}\tilde{\mathbf{h}} \in \mathbb{C}^{N_t \times 1}$, where $G_{\mathrm{c}} = \sqrt{N_t}$ is the antenna gain, and β_{c} is the path loss coefficient. The small-scale fading coefficient is modeled as $\tilde{\mathbf{h}} \sim \mathcal{CN}(0, \sigma^2\mathbf{I}_{N_t})$. Thus, the received signal $y(l)$ at the RN is given by

$$y(l) = \sqrt{\rho}\mathbf{h}^T\mathbf{w}_{\mathrm{s}}s_{\mathrm{s}}(l) + \sqrt{1-\rho}\mathbf{h}^T\mathbf{w}_{\mathrm{c}}s_{\mathrm{c}}(l) + n(l), \tag{4}$$

where $n(l)$ is the additive complex Gaussian noise with zero mean and variance σ^2, and $s_{\mathrm{s}}(l)$ and $s_{\mathrm{c}}(l)$ are the sensing and communication symbols, respectively. The received signal-to-interference-plus-noise ratio (SINR) for decoding the communication signal is then given by

$$\gamma = \frac{(1-\rho)|\mathbf{h}^H\mathbf{w}_{\mathrm{c}}|^2}{\rho|\mathbf{h}^H\mathbf{w}_{\mathrm{s}}|^2 + \sigma^2}. \tag{5}$$

As a result, the outage probability of the P-SAT ISAC system with threshold $\gamma_{\mathrm{th}}^{\mathrm{com}}$ is

$$P_\epsilon = \Pr\{\gamma < \gamma_{\mathrm{th}}^{\mathrm{com}}\} = \Pr\left\{\frac{(1-\rho)P|\mathbf{h}^H\mathbf{w}_{\mathrm{c}}|^2}{\rho P|\mathbf{h}^H\mathbf{w}_{\mathrm{s}}|^2 + \sigma_{\mathrm{com}}^2} < \gamma_{\mathrm{th}}^{\mathrm{com}}\right\}. \tag{6}$$

C. Defination of AoCS

As is known, AoI was defined as the time elapsed since the most recently received update is generated, ignoring sensing errors in fading environments. As such, traditional AoI cannot comprehensively characterize the timeliness of information in SAT ISAC systems, because in SAT ISAC, the RN may receive timely but incorrect information due to possible sensing errors. To efficiently measure the timeliness in SAT ISAC, the sensing errors should be taken into account. Therefore, we define the AoCS as a novel metric that captures the age of the latest correct sensed result received by the RN, which is expressed as $\Delta^{\mathrm{AoCS}}(t) = t - \mu(t)$, where $\mu(t)$ denotes the generation time of the latest successfully received correct sensed result at RN. The evolution of AoCS is described as

$$\Delta^{\mathrm{AoCS}}(t) = \begin{cases} 1, \text{ if } \mathrm{C(t-1)} = 1 \text{ and } \mathrm{D(t)} = 1, \\ \Delta^{\mathrm{AoCS}}(t-1) + 1, \text{otherwise}, \end{cases} \tag{7}$$

where $C(t-1) \in \{0,1\}$ and $D(t) \in \{0,1\}$ are binary variables, denoting whether the sensed result in slot $(t-1)$ is correct, and whether the communication is successful in slot t, respectively.

III. Analysis of PD, PFA, PCO and AoCS Minimization

A. PD, PFA and PCO of P-SAT ISAC

Lemma 1. *Based on LRT, the expressions for PD and PFA in the considered P-SAT ISAC network are given by*

$$P_{\mathrm{D}} \approx Q\left(\frac{\sigma^2\gamma_{\mathrm{th}}^{\mathrm{sen}} - LP\left(\rho|\mathbf{v}^H\mathbf{G}\mathbf{w}_{\mathrm{s}}|^2 + (1-\rho)|\mathbf{v}^H\mathbf{G}\mathbf{w}_{\mathrm{c}}|^2\right)}{\sqrt{2LP}\sigma\left(\sqrt{\rho}|\mathbf{v}^H\mathbf{G}\mathbf{w}_{\mathrm{s}}| + \sqrt{1-\rho}|\mathbf{v}^H\mathbf{G}\mathbf{w}_{\mathrm{c}}|\right)}\right), \tag{8}$$

$$P_{\mathrm{FA}} \approx Q\left(\frac{\sigma^2\gamma_{\mathrm{th}}^{\mathrm{sen}} + LP\left(\rho|\mathbf{v}^H\mathbf{G}\mathbf{w}_{\mathrm{s}}|^2 + (1-\rho)|\mathbf{v}^H\mathbf{G}\mathbf{w}_{\mathrm{c}}|^2\right)}{\sqrt{2LP}\sigma\left(\sqrt{\rho}|\mathbf{v}^H\mathbf{G}\mathbf{w}_{\mathrm{s}}| + \sqrt{1-\rho}|\mathbf{v}^H\mathbf{G}\mathbf{w}_{\mathrm{c}}|\right)}\right), \tag{9}$$

where $Q(\cdot)$ is the Gaussian Q-function with $Q(x) = \frac{1}{\sqrt{2\pi}}\int_x^\infty e^{-\frac{t^2}{2}}\,dt$.

Proof. Based on the PDF of $\mathbf{r}$, the distribution of the real part term $\Re(\mathbf{v}^H\mathbf{G}\mathbf{X}\mathbf{r}^H)$ in (2) is given by

$$\Re(\mathbf{v}^H\mathbf{G}\mathbf{X}\mathbf{r}^H) \sim \begin{cases} \mathcal{N}(0, \frac{1}{2}\sigma^2\|\mathbf{v}^H\mathbf{G}\mathbf{X}\|^2), & \mathcal{H}_0, \\ \mathcal{N}(\|\mathbf{v}^H\mathbf{G}\mathbf{X}\|^2, \frac{1}{2}\sigma^2\|\mathbf{v}^H\mathbf{G}\mathbf{X}\|^2), & \mathcal{H}_1. \end{cases} \tag{10}$$

Therefore, in the case of $\mathcal{H}_1$, PD is obtained by

$$\begin{aligned} &P_{\mathrm{D}}(\rho, \mathbf{w}_{\mathrm{c}}, \mathbf{w}_{\mathrm{s}}, \gamma_{\mathrm{th}}^{\mathrm{sen}}) = \Pr\left\{\ln \Lambda(\mathbf{r}) \geq \gamma_{\mathrm{th}}^{\mathrm{sen}} \mid \mathcal{H}_1\right\} \\ &= Q\left(\frac{\sigma^2\gamma_{\mathrm{th}}^{\mathrm{sen}} - \|\mathbf{v}^H\mathbf{G}\mathbf{X}\|^2}{\sqrt{2}\sigma\|\mathbf{v}^H\mathbf{G}\mathbf{X}\|}\right) = Q\left(\frac{\sigma^2\gamma_{\mathrm{th}}^{\mathrm{sen}} - \|\Psi\|^2}{\sqrt{2}\sigma\|\Psi\|}\right). \end{aligned} \tag{11}$$

where $\Psi = \sqrt{\rho P}\mathbf{v}^H\mathbf{G}\mathbf{w}_{\mathrm{s}}\mathbf{s}_{\mathrm{s}}^H + \sqrt{(1-\rho)P}\mathbf{v}^H\mathbf{G}\mathbf{w}_{\mathrm{c}}\mathbf{s}_{\mathrm{c}}^H$. When L is sufficiently large, the sensing signal can be approximated by its statistical expectation. Since each element in $\mathbf{s}_{\mathrm{s}}$ and $\mathbf{s}_{\mathrm{c}}$ is i.i.d., we have $\mathbf{s}_{\mathrm{s}}^H\mathbf{s}_{\mathrm{s}} \approx \mathbb{E}\{\mathbf{s}_{\mathrm{s}}^H\mathbf{s}_{\mathrm{s}}\} = L$ and $\mathbf{s}_{\mathrm{s}}^H\mathbf{s}_{\mathrm{c}} = 0$. As a result, Eq. (11) is approximated to be (8). In the case of $\mathcal{H}_0$, PFA is obtained by

$$\begin{aligned} &P_{\mathrm{FA}}(\rho, \mathbf{w}_{\mathrm{c}}, \mathbf{w}_{\mathrm{s}}, \gamma_{\mathrm{th}}^{\mathrm{sen}}) = \Pr\left\{\ln \Lambda(\mathbf{r}) \geq \gamma_{\mathrm{th}}^{\mathrm{sen}} \mid \mathcal{H}_0\right\} \\ &= Q\left(\frac{\sigma^2\gamma_{\mathrm{th}}^{\mathrm{sen}} + \|\mathbf{v}^H\mathbf{G}\mathbf{X}\|^2}{\sqrt{2}\sigma\|\mathbf{v}^H\mathbf{G}\mathbf{X}\|}\right) = Q\left(\frac{\sigma^2\gamma_{\mathrm{th}}^{\mathrm{sen}} + \|\Psi\|^2}{\sqrt{2}\sigma\|\Psi\|}\right). \end{aligned} \tag{12}$$

Similarly, Eq. (12) is approximated to be (9). □

Lemma 2. *In Rayleigh fading, the PCO, denoted as P_ϵ, is*

$$P_\epsilon(\rho, \mathbf{w}_\mathrm{c}, \mathbf{w}_\mathrm{s}, \gamma_\mathrm{th}^\mathrm{com}) = u(\gamma_\mathrm{th}^\mathrm{com}\sigma_\mathrm{com}^2) - \sum_{l=1}^{N_t} \frac{\lambda_l^{N_t}}{\prod_{i=1, i\neq l}^{N_t}(\lambda_l - \lambda_i)} \cdot \frac{1}{|\lambda_l|} e^{-\frac{\gamma_\mathrm{th}^\mathrm{com}\sigma_\mathrm{com}^2}{\lambda_l}} u\left(\frac{\gamma_\mathrm{th}^\mathrm{com}\sigma_\mathrm{com}^2}{\lambda_l}\right), \tag{13}$$

where $\Phi = (1-\rho)P\mathbf{w}_\mathrm{c}\mathbf{w}_\mathrm{c}^H - \gamma_\mathrm{th}^\mathrm{com}\rho P\mathbf{w}_\mathrm{s}\mathbf{w}_\mathrm{s}^H$, λ_l is the l-th eigenvalue of the matrix Φ and $u(\cdot)$ is the unit step function.

Proof. In Rayleigh fading, P_ϵ can be characterized based on the distribution of Hermitian quadratic forms over central complex Gaussian vectors [14]. Similar to the proof in [14], the detailed derivation is omitted for brevity. □

B. Analysis of the expected AoCS

As the instantaneous AoCS reflects only the timeliness in a specific slot and cannot capture long-term performance in dynamic systems, we use the expected AoCS to evaluate the system performance, which is defined as

$$\bar{\Delta}^\mathrm{AoCS} = \mathbb{E}_t[\Delta^\mathrm{AoCS}(t)] = \sum_{i=1}^{\infty} i \cdot \Pr\{\Delta^\mathrm{AoCS}(t) = i\}. \tag{14}$$

Lemma 3. *In the considered P-SAT ISAC, $\bar{\Delta}^\mathrm{AoCS}$ is*

$$\bar{\Delta}^\mathrm{AoCS} = \frac{p+q}{q(1-P_\epsilon)(1-P_\mathrm{FA}) + p(1-P_\epsilon)P_\mathrm{D}}. \tag{15}$$

Proof. $\Pr\{\Delta^\mathrm{AoCS}(t) = i\}$ can be expressed as the probability that all of the first $(i-1)$ attempts result in unsuccessful joint sensing–communication events while the i-th attempt yields a successful event, which is given by

$$\Pr\{\Delta^\mathrm{AoCS}(t) = i\} = \prod_{k=1}^{i-1}(1 - \Pr\{C(t-k-1) = 1, D(t-k) = 1\}) \cdot \Pr\{C(t-1) = 1, D(t) = 1\}, \quad i = 2, 3 \ldots. \tag{16}$$

Since for long-term observations, the system operates stably, the noise distribution and channel distribution in the system do not change with time. Accordingly, $\Pr\{C(t-1) = 1, D(t) = 1\}$ is identical for all t. Consequently, by substituting (16) into (14), we have that

$$\bar{\Delta}^\mathrm{AoCS} = \frac{1}{\Pr\{C(t-1) = 1, D(t) = 1\}}. \tag{17}$$

Moreover, for the sensed data obtained in the $(t-1)$-th slot, its associated sensing and communication operations are performed in two orthogonal time slots, so the events $\{C(t-1) = 1\}$ and $\{D(t) = 1\}$ are independent, leading to $\Pr\{C(t-1) = 1, D(t) = 1\} = \Pr\{C(t-1) = 1\}\Pr\{D(t) = 1\}$. Then, $\Pr\{C(t-1) = 1\}\Pr\{D(t) = 1\}$ can be further derived via the total probability law as follows:

$$\begin{aligned}
&\Pr\{C(t-1) = 1\}\Pr\{D(t) = 1\} \\
&= \Pr\{D(t) = 1\}(\Pr\{\{C(t-1) = 1 \mid X(t) = \mathcal{H}_0\}\}\Pr\{X(t) \\
&= \mathcal{H}_0\} + P\{C(t-1) = 1 \mid X(t) = \mathcal{H}_1\}\Pr\{X(t) = \mathcal{H}_1\}) \\
&= (1-P_\epsilon)((1-P_\mathrm{FA})\Pr\{X(t) = \mathcal{H}_0\} + P_\mathrm{D}\Pr\{X(t) = \mathcal{H}_1\}).
\end{aligned} \tag{18}$$

Over long-term evolution, $\Pr\{X(t) = \mathcal{H}_0\}$ and $\Pr\{X(t) = \mathcal{H}_1\}$ converge to the stationary distribution of the Markov process, which is given by

$$\Pr\{X(t) = H_0\} = \tfrac{q}{p+q}, \quad \Pr\{X(t) = H_1\} = \tfrac{p}{p+q}. \tag{19}$$

Substituting (18) and (19) into (17) yields (15). □

C. Problem formulation and solution

To explore the lower-bound of AoCS in the P-SAT ISAC system, we formulate an AoCS minimization problem by optimizing the power splitting factor ρ, which is

$$\mathrm{P}_0 : \underset{\rho}{\text{minimize}} \quad \bar{\Delta}^\mathrm{AoCS}, \quad \text{subject to} \quad 0 \le \rho \le 1. \tag{20}$$

where $0 \le \rho \le 1$ specifies the feasible range of ρ.

Due to the Gaussian Q-functions and eigenvalue-based terms in (10)–(12), the objective function exhibits a semi-closed dependence on ρ, preventing a closed-form global optimum. To achieve the minimum $\bar{\Delta}^{*\mathrm{AoCS}}$, a one-dimensional linear search is performed with a step size of $\Delta\rho$, which has the computational complexity of $\mathcal{O}\left(\frac{1}{\Delta\rho}\right)$.

IV. NUMERICAL RESULTS AND DISCUSSION

The simulation parameters are as follows. The number of transmit antennas is set to $N_t = 4$ and the number of receive antennas is set to $N_r = 4$. The transmit power is $P = 10$ dBm. The transmission sequence length is $L = 100$, and the RCS coefficient is 1. The communication noise power is -114 dBm, and the sensing noise power is -156 dBm. The distance from the RN to the MBS is $d_\mathrm{RN} = 100$ m with an azimuth angle of $\theta_\mathrm{RN} = \pi/4$, and the distance from the target to the MBS is $d_\mathrm{tar} = 100$ m with an azimuth angle of $\theta_\mathrm{tar} = \pi/2$. The path loss exponent is $\alpha = 4$. The probability that the target remains present in the next time slot is $p = 0.4$, and the probability that the target remains absent is $q = 0.5$. The search step size is set to $\Delta\rho = 0.0001$.

Fig. 3(a) and Fig. 3(b) show P_D, P_FA, and P_ϵ w.r.t. $\gamma_\mathrm{th}^\mathrm{com}$ and $\gamma_\mathrm{th}^\mathrm{sen}$ with different ρ. To validate the correctness of the theoretical analysis, we conduct Monte Carlo simulations, based on 100,000 independent simulation trials for each configuration. As shown in the Fig. 3, the theoretical results of P_D, P_FA, and P_ϵ match perfectly with the Monte Carlo simulations. Moreover, Fig. 4(a)–(c) show that increasing ρ leads to higher P_D, lower P_FA, and higher P_ϵ. This reflects the fundamental trade-off. That is, allocating more power to sensing enhances echo signal strength, improving detection accuracy, but simultaneously reduces the power available for communication, and also introduces additional interference, both of which further make P_ϵ increase. Moreover, it is seen from Fig. 4(a) and Fig. 4(b) that P_D decreases monotonically while P_FA decreases with increasing $\gamma_\mathrm{th}^\mathrm{sen}$, because $\gamma_\mathrm{th}^\mathrm{sen}$ serves as the decision threshold for target detection and the higher threshold makes it harder for signals to exceed the decision boundary, reducing P_D, yet also lowering P_FA. This indicates that the system's sensitivity to target detection can be adjusted by tuning $\gamma_\mathrm{th}^\mathrm{sen}$. In Fig. 4(c), as $\gamma_\mathrm{th}^\mathrm{com}$ increases, $P\epsilon$ rises

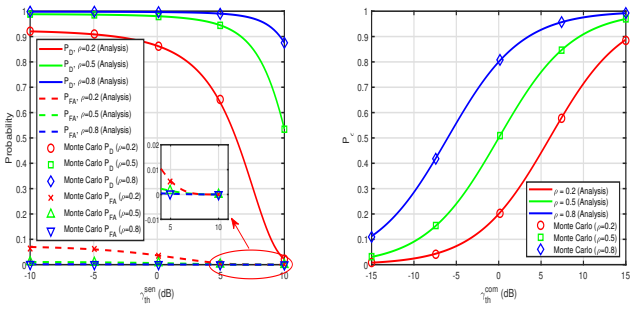

(a) (b)

Fig. 3: Theoretical analysis vs. Monte Carlo results.

monotonically, since a higher $\gamma_{\rm th}^{\rm com}$ increases the likelihood of outage.

Fig. 5(a) shows the effect of $\gamma_{\rm th}^{\rm sen}$ and $\gamma_{\rm th}^{\rm com}$ on the minimum achievable $\bar{\Delta}^{*\rm AoCS}$. When $\gamma_{\rm th}^{\rm com}$ is below 0, variations in $\gamma_{\rm th}^{\rm sen}$ have little influence on $\bar{\Delta}^{*\rm AoCS}$. When $\gamma_{\rm th}^{\rm com}$ is exceeds 0, $\bar{\Delta}^{\rm AoCS}$ decreases as $\gamma_{\rm th}^{\rm sen}$ increases, because to minimize $\bar{\Delta}^{\rm AoCS}$, more power will be allocated to communication, making sensing increasingly resource-constrained. As a result, $\gamma_{\rm th}^{\rm sen}$ exerts a stronger influence on both $P_{\rm D}$ and $P_{\rm FA}$. A higher sensing threshold suppresses false alarms and enhances the correctness of sensed results, thereby reducing the $\bar{\Delta}^{*\rm AoCS}$.

Fig. 5(b) compares the achievable $\bar{\Delta}^{\rm AoCS}$ of our proposed P-SAT ISAC to three baselines, i.e., A-SAT ISAC, MB-SAT ISAC, and P-SAT ISAC with equal power splitting. In A-SAT ISAC, sensing and communication are performed in alternating time slots in [4] (also referred to as the R&C mode in [12]). In MB-SAT ISAC, the MBS performs sensing using the one single beam in [4] (also referred to as the communication-only mode in [2]). In P-SAT ISAC with equal power splitting, the sensing and communication are performed with equal power splitting, i.e., $\rho = 0.5$. As shown in Fig. 5(b), the values of $\bar{\Delta}^{\rm AoCS}$ increase with the increasement of $\gamma_{\rm th}^{\rm com}$, since a higher threshold requires a stronger received SINR for successful transmission, increasing PCO, thereby degrading timeliness. Compared with the A-SAT ISAC, our proposed P-SAT ISAC achieves a 38.97% reduction in $\bar{\Delta}^{\rm AoCS}$, demonstrating that the pipelined sensing and communication framework's efficiency in enhance system timeliness. Moreover, compared with the MB-SAT ISAC, P-SAT ISAC yields about 18.82% reduction in $\bar{\Delta}^{\rm AoCS}$, which stems from the individual beam design and efficient power splitting optimization. In addition, compared with P-SAT ISAC with equal power splitting, the performance gap widens as $\gamma_{\rm th}^{\rm com}$ increases, indicating that the power splitting factor should be dynamically optimized to enhance timeliness.

V. CONCLUSION

This paper studied the SAT ISAC network. A new metric, AoCS, was proposed to capture the overall timeliness of the SAT process. To minimize the AoCS, an efficient P-SAT ISAC paradigm was presented. Theoretical expressions of the long-term expected AoCS was derived and the minimum expected AoCS was found. Simulation results validate the theoretical analysis and demonstrate the efficiency of the pipelined sensing and communication paradigm in enhancing system timeliness.

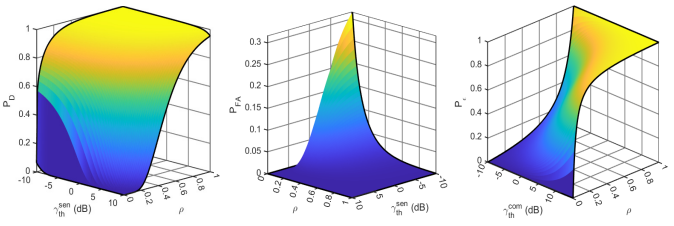

(a) (b) (c)

Fig. 4: $P_{\rm D}$, $P_{\rm FA}$, and P_ϵ vs. the respective thresholds and ρ.

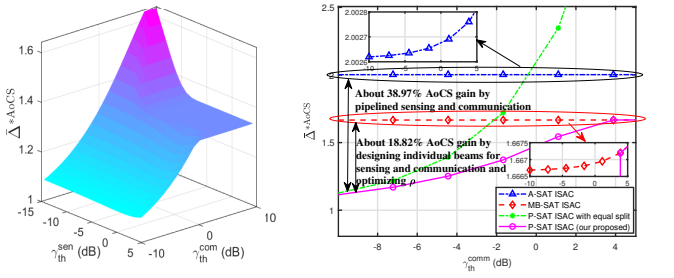

(a) (b)

Fig. 5: (a) Minimum achievable $\bar{\Delta}^{*\rm AoCS}$ vs. $\gamma_{\rm th}^{\rm sen}$ and $\gamma_{\rm th}^{\rm com}$. (b) Achievable $\bar{\Delta}^{\rm AoCS}$ comparison.

REFERENCES

[1] W. Saad, M. Bennis, and M. Chen, "A vision of 6G wireless systems: Applications, trends, technologies, and open research problems," *IEEE Network*, vol. 34, no. 3, pp. 134–142, May/Jun. 2020.

[2] H. Ke *et al.*, "Rate splitting and beamforming design for RIS-assisted rsma-enhanced ISAC networks," *IEEE Wireless Commun. Lett.*, vol. 14, no. 6, pp. 1738–1742, Jun. 2025.

[3] A. Liu *et al.*, "A survey on fundamental limits of integrated sensing and communication," *IEEE Commun. Surv. Tutorials*, vol. 24, no. 2, pp. 994–1034, Secondquarter 2022.

[4] F. Dong *et al.*, "Communication-assisted sensing in 6G networks," *IEEE J. Sel. Areas Commun.*, vol. 43, no. 4, pp. 1371–1386, Apr. 2025.

[5] Q. Zhang *et al.*, "Design and performance evaluation of joint sensing and communication integrated system for 5G mmwave enabled CAVs," *IEEE J. Sel. Top. Signal Process.*, vol. 15, no. 6, pp. 1500–1514, 2021.

[6] Y. Zhang *et al.*, "Statistical aoi guarantee optimization for supporting xurllc in ISAC-enabled V2I networks," *arXiv:2408.00381*, 2024.

[7] Y. Ge *et al.*, "Aoi-minimal power adjustment in RF-EH-powered industrial IoT networks: A soft actor-critic-based method," *IEEE Trans. Mob. Comput.*, vol. 23, no. 9, pp. 8729–8741, Sep. 2024.

[8] H. Mei *et al.*, "Aoi minimization for air-ground integrated sensing and communication networks with jamming attack," *IEEE Trans. Veh. Technol.*, vol. 74, no. 8, pp. 12 776–12 790, 2025.

[9] Z. Liu *et al.*, "Joint sensing and age of information optimization for energy constrained UAV assisted integrated sensing, calculation and communication," *IEEE Trans. Wireless Commun.*, vol. 24, no. 5, pp. 4440–4453, May 2025.

[10] X. Li *et al.*, "Detecting unauthorized drones with cell-free integrated sensing and communication," *arXiv:2501.15227*, 2025.

[11] B. K. Chalise, M. G. Amin, and B. Himed, "Performance tradeoff in a unified passive radar and communications system," *IEEE Signal Process Lett.*, vol. 24, no. 9, pp. 1275–1279, Sep. 2017.

[12] J. An *et al.*, "Fundamental detection probability vs. achievable rate tradeoff in integrated sensing and communication systems," *IEEE Trans. Wireless Commun.*, vol. 22, no. 12, pp. 9835–9853, Dec. 2023.

[13] A. Maatouk, S. Kriouile, M. Assaad, and A. Ephremides, "The age of incorrect information: A new performance metric for status updates," *IEEE/ACM Trans. Networking*, vol. 28, no. 5, pp. 2215–2228, Oct. 2020.

[14] T. Y. Al-Naffouri *et al.*, "On the distribution of indefinite quadratic forms in gaussian random variables," *IEEE Trans. Commun.*, vol. 64, no. 1, pp. 153–165, Jan. 2015.